

On the mixed spin-scalar coupling approach in dark matter search

V.A.Bednyakov¹ and H.V. Klapdor-Kleingrothaus²

¹ Laboratory of Nuclear Problems, Joint Institute for Nuclear Research, 141980 Dubna, Russia. E-mail: Vadim.Bednyakov@jinr.ru

² Max-Planck-Institut für Kernphysik, Postfach 103980, D-69029, Heidelberg, Germany. E-mail: H.Klapdor@mpi-hd.mpg.de

Abstract. To avoid misleading discrepancies between results of different dark matter search experiments as well as between the data and SUSY calculations it is in general preferable to use a mixed spin-scalar coupling approach in which spin-independent and spin-dependent WIMP-nucleon couplings are *both* non-zero. On the other hand one may, however, to safely neglect the subdominant spin WIMP-nucleon contribution in comparison with the spin-independent one in analysis of data from experiments with heavy enough non-zero-spin target nuclei.

The mixed coupling approach is applied to estimate future prospects of experiments with the odd-neutron high-spin isotope ⁷³Ge.

1 Introduction

In many experiments one tries to detect directly relic dark matter (DM) Weakly Interacting Massive Particles (WIMPs) χ via their elastic scattering on a target nucleus (A, Z) . The nuclear recoil energy E_R ($E_R \sim 10^{-6} m_\chi \sim$ few keV) is measured. The expected differential event rate has the form [1]–[8]:

$$\frac{dR}{dE_R} = N_t \frac{\rho_\chi}{m_\chi} \int_{v_{\min}}^{v_{\max}} dv f(v) v \frac{d\sigma}{dq^2}(v, q^2), \quad E_R = q^2/(2M_A). \quad (1)$$

Here, $v_{\min} = \sqrt{M_A E_R / 2\mu_A^2}$, $v_{\max} = v_{\text{esc}} \approx 600$ km/s, $\mu_A = \frac{m_\chi M_A}{m_\chi + M_A}$; $f(v)$ is the distribution of χ -particles in the solar vicinity, N_t is the number density of target nuclei. M_A denotes the target nuclear mass, the dark matter density is usually assumed to be $\rho_\chi = 0.3$ GeV/cm³. The χ -nucleus elastic scattering cross section for non-zero-spin ($J \neq 0$) nuclei is a sum of the spin-independent (SI, or scalar) and spin-dependent (SD, axial) terms [9, 10, 11, 12]:

$$\frac{d\sigma^A}{dq^2}(v, q^2) = \frac{\sigma_{\text{SD}}^A(0)}{4\mu_A^2 v^2} F_{\text{SD}}^2(q^2) + \frac{\sigma_{\text{SI}}^A(0)}{4\mu_A^2 v^2} F_{\text{SI}}^2(q^2). \quad (2)$$

For $q = 0$ the nuclear SD and SI cross sections take the forms

$$\sigma_{\text{SI}}^A(0) = \frac{\mu_A^2}{\mu_p^2} A^2 \sigma_{\text{SI}}^p(0), \quad (3)$$

$$\sigma_{\text{SD}}^A(0) = \frac{4\mu_A^2}{\pi} \frac{(J+1)}{J} \left\{ a_p \langle \mathbf{S}_p^A \rangle + a_n \langle \mathbf{S}_n^A \rangle \right\}^2 \quad (4)$$

$$= \frac{\mu_A^2}{\mu_p^2} \frac{4}{3} \frac{J+1}{J} \sigma_{\text{SD}}(0) \left\{ \langle \mathbf{S}_p^A \rangle \cos \theta + \langle \mathbf{S}_n^A \rangle \sin \theta \right\}^2. \quad (5)$$

The dependence on effective χ -quark scalar \mathcal{C}_q and axial \mathcal{A}_q couplings and on the spin $\Delta_q^{(p,n)}$ and the mass $f_q^{(p,n)}$ structure of *nucleons* enter into these formulas via the zero-momentum-transfer proton and neutron SI and SD cross sections ($\mu_n^2 = \mu_p^2$ is assumed):

$$\sigma_{\text{SI}}^p(0) = 4 \frac{\mu_p^2}{\pi} c_0^2, \quad \sigma_{\text{SD}}^{p,n}(0) = 12 \frac{\mu_{p,n}^2}{\pi} a_{p,n}^2; \quad (6)$$

$$c_0 = c_0^{p,n} = \sum_q \mathcal{C}_q f_q^{(p,n)}, \quad a_p = \sum_q \mathcal{A}_q \Delta_q^{(p)}, \quad a_n = \sum_q \mathcal{A}_q \Delta_q^{(n)}. \quad (7)$$

The effective spin WIMP-nucleon cross section $\sigma_{\text{SD}}(0)$ and the coupling mixing angle θ [13, 14] were introduced in (5):

$$\sigma_{\text{SD}}(0) = \frac{\mu_p^2}{\pi} \frac{4}{3} \left[a_p^2 + a_n^2 \right], \quad \tan \theta = \frac{a_n}{a_p}. \quad (8)$$

The factors $\Delta_q^{(p,n)}$, which parametrize the quark spin content of the nucleon, are defined as $2\Delta_q^{(n,p)} s^\mu \equiv \langle p, s | \bar{\psi}_q \gamma^\mu \gamma_5 \psi_q | p, s \rangle_{(p,n)}$. The $\langle \mathbf{S}_{p(n)}^A \rangle$ is the total spin of protons (neutrons) averaged over all A nucleons of the nucleus (A, Z). In the simplest case the SD and SI nuclear form-factors

$$F_{\text{SD,SI}}^2(q^2) = \frac{S_{\text{SD,SI}}^A(q^2)}{S_{\text{SD,SI}}^A(0)} \quad (9)$$

have a Gaussian form (see, for example, [15]). The spin-dependent structure function $S_{\text{SD}}^A(q)$ in terms of isoscalar $a_0 = a_n + a_p$ and isovector $a_1 = a_p - a_n$ effective couplings has the form [11, 12]:

$$S_{\text{SD}}^A(q) = a_0^2 S_{00}(q) + a_1^2 S_{11}(q) + a_0 a_1 S_{01}(q). \quad (10)$$

2 One-coupling dominance approach

One can see from (2)–(7) that the direct dark matter search experiments supply us with only three different constants for the underlying SUSY theory from non-observation of a DM signal (c_0 , a_p and a_n , or $\sigma_{\text{SI}}^p(0)$, $\sigma_{\text{SD}}^p(0)$ and $\sigma_{\text{SD}}^n(0)$), provided the DM particle is the lightest SUSY particle (LSP) neutralino [16]. These constraints are traditionally presented in the form of sets

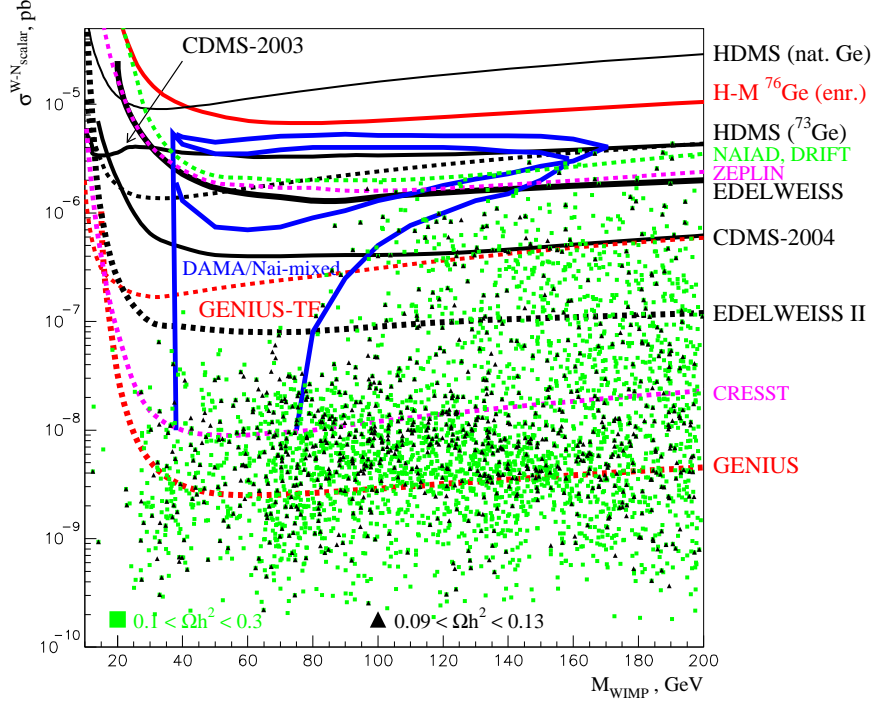


Fig. 1. WIMP-nucleon cross section limits in pb for spin-independent (scalar) interactions as a function of the WIMP mass in GeV. Shown are contour lines for some of the present experimental limits (solid lines) and some of projected experiments (dashed lines). All curves are obtained in the one-coupling dominance approach with $\sigma_{\text{SD}} = 0$. For example, the closed DAMA/NaI contour corresponds to complete neglect of SD WIMP-nucleon interaction. Only the open DAMA contour is obtained in [13] with the assumption that $\sigma_{\text{SD}} = 0.08 \text{ pb} > 0$. From [17].

of exclusion curves for the spin-independent (scalar) nucleon-WIMP (Fig. 1), spin-dependent (axial) proton-WIMP (Fig. 2) and spin-dependent neutron-WIMP cross sections (Fig. 3) as functions of the WIMP mass. From (4) one can also see that contrary to the SI case (3) both proton $\langle \mathbf{S}_p^A \rangle$ and neutron $\langle \mathbf{S}_n^A \rangle$ spin contributions simultaneously enter into formula (4) for the SD WIMP-nucleus cross section $\sigma_{\text{SD}}^A(0)$. Nevertheless, for the most interesting isotopes either $\langle \mathbf{S}_p^A \rangle$ or $\langle \mathbf{S}_n^A \rangle$ dominates ($\langle \mathbf{S}_{n(p)}^A \rangle \ll \langle \mathbf{S}_{p(n)}^A \rangle$) [17, 18].

In earlier considerations [3, 10, 15, 19, 20, 21] one reasonably assumed that the nuclear spin was carried by the “odd” unpaired group of protons or neutrons and only one of either $\langle \mathbf{S}_n^A \rangle$ or $\langle \mathbf{S}_p^A \rangle$ was non-zero. In this case all possible non-zero-spin target nuclei can be classified into n-odd and p-odd groups. Following this classification, the current experimental situation for the spin-dependent WIMP-**proton** and WIMP-**neutron** cross sections are naturally presented separately in Fig. 2 and Fig. 3. The DAMA/NaI-7 con-

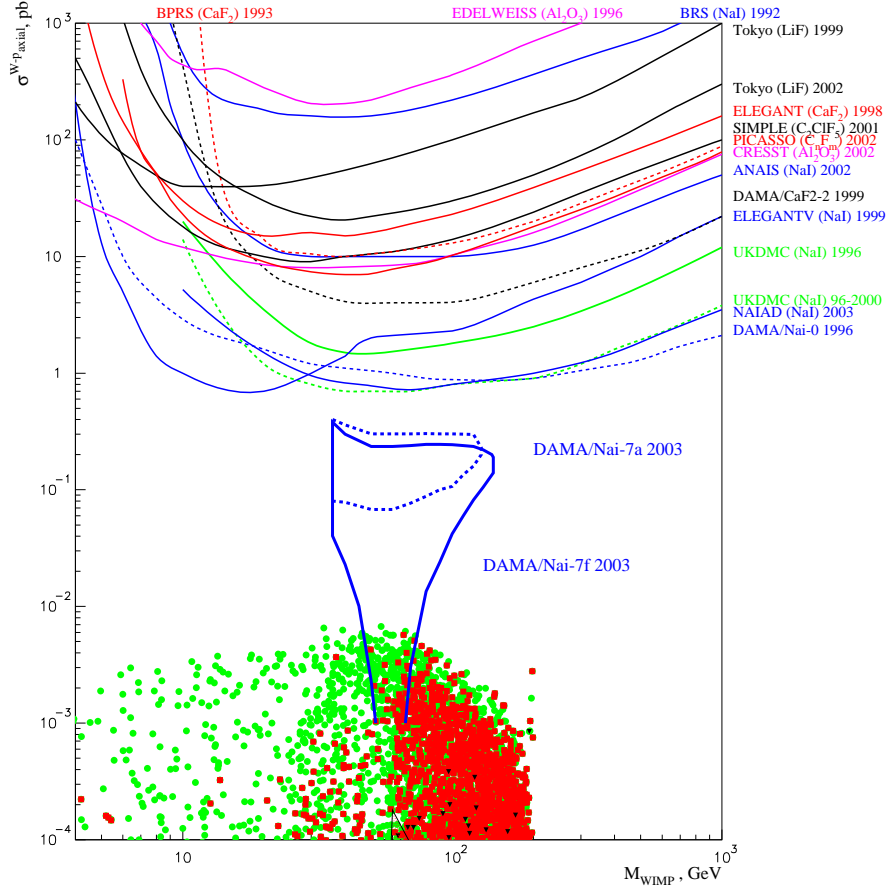


Fig. 2. Exclusion curves for the spin-dependent WIMP-proton cross sections (σ_{SD}^p as a function of the WIMP mass). All curves, except the NAIAD and Tokio-LiF, are obtained in the one-coupling dominance approach with $\sigma_{SI} = 0$ and $\sigma_{SD}^n = 0$. DAMA/NaI-7a(f) contours for the WIMP-proton SD interaction in ^{127}I are obtained on the basis of the positive signature of annual modulation within the framework of the mixed scalar-spin coupling approach [13, 14]. From [17].

tours for the WIMP-proton SD interaction (dominating in ^{127}I) obtained on the basis of the positive signature of the annual modulation (closed contour) [13] and within the mixed coupling framework (open contour) [14] are also presented in Fig. 2. Similarly, the DAMA/NaI-7 [13] contours for the WIMP-neutron SD interaction (subdominant in ^{127}I) are given in Fig. 3. One can also expect some exclusion curves for the SD cross section from the CDMS [22] and EDELWEISS [23] experiments with natural-germanium bolometric detectors (due to a small Ge-73 admixture). The scatter plots for the SD

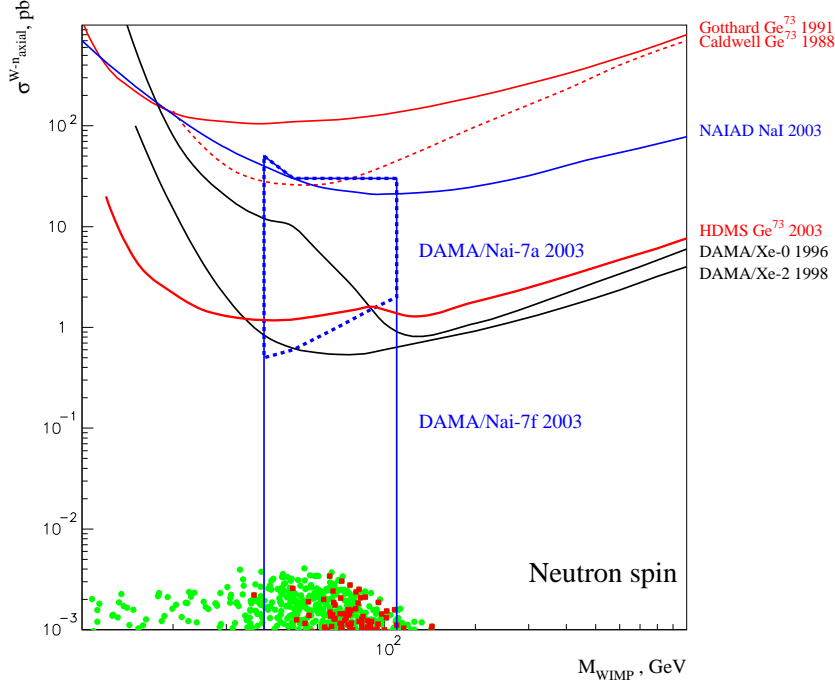


Fig. 3. Exclusion curves for the spin-dependent WIMP-neutron cross sections (σ_{SD}^n versus the WIMP mass). DAMA/NaI-7a(f) contours for the WIMP-neutron SD interaction (subdominating in ^{127}I) are obtained from the relevant figures of [13, 14]. Note that the NAIAD curve here corresponds to the WIMP-neutron SD interaction subdominant for ^{127}I . The WIMP-proton SD interaction dominates for this nucleus. The curve was obtained in the approach of [24]. It is much weaker in comparison with the both DAMA/Xe and HDMS curves. From [17].

LSP-proton and LSP-neutron cross sections calculated in the effMSSM from [17] are also given in Figs. 1–3.

We would like to stress that the calculated scatter plots for σ_{SD}^p (Fig. 2) are obtained without any assumption of $\sigma_{SD}^n = 0$ (and $\sigma_{SI}^p = 0$), but the experimental exclusion curves for σ_{SD}^p were traditionally extracted from the data with the spin-neutron (and scalar) contribution fully neglected, i.e. under the assumption that $\sigma_{SD}^n = 0$ (and $\sigma_{SI}^p = 0$). This **one-spin-coupling dominance scheme** (always used before new approaches were proposed in [24] and in [13, 25, 26]) gave a bit too pessimistic exclusion curves, but allowed direct comparison of sensitivities for different experiments. More stringent constraints on σ_{SD}^p can be obtained [24, 13, 25, 26] by assuming both $\sigma_{SD}^p \neq 0$ and $\sigma_{SD}^n \neq 0$ (although the contribution of the neutron spin is usually very small because $\langle \mathbf{S}_n^A \rangle \ll \langle \mathbf{S}_p^A \rangle$). Therefore a direct comparison of

the old-fashioned exclusion curves with the new ones could in principle be misleading.

The same conclusion on the one-coupling dominance approach to a great extent concerns [13, 26] the direct comparison of the *old* SI exclusion curves (obtained with zero SD contribution, $\sigma_{\text{SD}} = 0$) with the *new* SI exclusion curves (obtained with non-zero SD contribution, $\sigma_{\text{SD}} > 0$) as well as with the results of the SUSY calculations. One can see from Fig. 1 that the *new-type* DAMA/NaI open contour (when $\sigma_{\text{SD}} > 0$) is in agreement with the best exclusion curves of the CDMS and EDELWEISS as well as with SUSY calculations. One knows that both these experiments have natural germanium (almost pure spinless) as a target and therefore have no sensitivity to the spin-dependent WIMP-nucleon couplings (for them $\sigma_{\text{SD}} \equiv 0$). Therefore, these experiments exclude only the pure SI interpretation of the DAMA annual modulation signal [22, 27, 28, 29, 30]. The statement that this DAMA result is *completely* excluded by the results of these cryogenic experiments and is inconsistent with the SUSY interpretation (see, for example, [31]) is simply wrong (see also discussions in [28, 32]).

The event-by-event CDMS and EDELWEISS background discrimination (via simultaneous charge and phonon signal measurements) is certainly very important. Nevertheless the DAMA annual signal modulation is one of a few available *positive* signatures of WIMP-nucleus interactions and the importance of its observation goes far beyond a simple background reduction. Therefore, to completely exclude the DAMA result, a new experiment, being indeed sensitive to the modulation signal, would have to exclude this modulation signal on the basis of the same or much better statistics.

Furthermore, taking seriously the positive DAMA result together with the negative results of the CDMS and EDELWEISS as well as the results of [33] one can arrive at a conclusion about simultaneous existence and importance of both SD and SI WIMP-nucleus interactions.

3 Mixed spin-scalar WIMP-nucleon couplings

More accurate calculations of spin nuclear structure (see a review in [18]) demonstrate that contrary to the simplified odd-group approach both $\langle \mathbf{S}_p^A \rangle$ and $\langle \mathbf{S}_n^A \rangle$ differ from zero, but nevertheless one of these spin quantities always dominates ($\langle \mathbf{S}_p^A \rangle \ll \langle \mathbf{S}_n^A \rangle$, or $\langle \mathbf{S}_n^A \rangle \ll \langle \mathbf{S}_p^A \rangle$). *If together* with the dominance like $\langle \mathbf{S}_{p(n)}^A \rangle \ll \langle \mathbf{S}_{n(p)}^A \rangle$ one would have WIMP-proton and WIMP-neutron couplings of the same order of magnitude (*not* $a_{n(p)} \ll a_{p(n)}$), the situation could look like that in the odd-group model and one could safely (at the current level of accuracy) neglect subdominant spin contribution in the data analysis. Indeed, very large or very small ratios $\sigma_p/\sigma_n \sim a_p/a_n$ would correspond to the neutralinos which are extremely pure gauginos. In this case Z -boson exchange in the SD interactions is absent and only sfermions make

contributions to the SD cross sections. This is a very particular case which is also currently in disagreement with the experiments. We have checked the relation $|a_n|/|a_p| \approx O(1)$ for large LSP masses in [34]. For relatively low LSP masses $m_\chi < 200$ GeV in effMSSM [35]–[41] the a_n -to- a_p ratio is located within the bounds [17]:

$$0.5 < \left| \frac{a_n}{a_p} \right| < 0.8. \quad (11)$$

Therefore the couplings are almost the same and one can quite safely use the *clear* “old” n-odd and p-odd group classification of non-zero-spin targets and neglect, for example, the $\langle \mathbf{S}_p^A \rangle$ -spin contribution in the analysis of the DM data for a nuclear target with $\langle \mathbf{S}_p^A \rangle \ll \langle \mathbf{S}_n^A \rangle$. Furthermore, when one compares in the same figure the exclusion curve for SD WIMP-proton coupling obtained without the subdominant SD WIMP-neutron contribution (all curves in Fig. 2 except the NAIAD one [42] and the Tokyo-LiF one [43]) with the curve from the approach of [24], when the subdominant contribution is included (the NAIAD and Tokyo-LiF curves in Fig. 2), one “*artificially*” improves the sensitivity of the *latter* curves (NAIAD or Tokyo-LiF) in comparison with the former ones. For the sake of consistency and reliable comparisons, one should coherently recalculate all previous curves in the new manner [13].

We note that it looks like the SI contribution is completely ignored in the SIMPLE experiment [44, 45] and the DM search with NaF bolometers [46]. Although ^{19}F has the best properties for investigation of WIMP-nucleon spin-dependent interactions (see, for example, [47]) it is not obvious that one should completely ignore spin-independent WIMP coupling with fluorine. For

example, in the relation $\sigma^A \sim \sigma_{\text{SD}}^{A,p} \left[\frac{\sigma_{\text{SI}}^A}{\sigma_{\text{SD}}^{A,p}} + \left(1 + \sqrt{\frac{\sigma_{\text{SD}}^{A,n}}{\sigma_{\text{SD}}^{A,p}}} \right)^2 \right]$, which follows

from (3)–(5), it is not a priori clear that $\frac{\sigma_{\text{SI}}^A}{\sigma_{\text{SD}}^{A,p}} \ll \frac{\sigma_{\text{SD}}^{A,n}}{\sigma_{\text{SD}}^{A,p}}$, i.e. the SI WIMP-nucleus interaction is much weaker than the subdominant SD WIMP-nucleus one. At least for isotopes with an atomic number $A > 50$ [1, 8] to neglect the SI contribution would be a larger mistake than to neglect the subdominant SD WIMP-neutron contribution, when the SD WIMP-proton interaction dominates, at the current level of sensitivity of DM experiments [35, 48]. From measurements with ^{73}Ge one can extract, following [24], not only the dominant constraint for the WIMP-nucleon coupling a_n (or σ_{SD}^n) but also the constraint for the subdominant WIMP-proton coupling a_p (or σ_{SD}^p). Nevertheless, the latter constraint will be much weaker in comparison with the constraints from p-odd target nuclei, like ^{19}F or ^{127}I . This fact is illustrated by the “weak” NAIAD (NaI, 2003) curve in Fig. 3, which corresponds to the subdominant WIMP-neutron spin contribution extracted from the p-odd nucleus ^{127}I .

Therefore we would like to note that the “old” odd-group-based approach to analysis of the SD data from experiments with heavy enough targets (for

example, Ge-73) is still quite suitable, especially when it is not obvious that (both) spin couplings dominate over the scalar one.

The approach of Bernabei et al. [13, 14] looks more appropriate for the mixed spin-scalar coupling data presentation, and is based on introduction of the effective SD nucleon cross section $\sigma_{\text{SD}}(0)$ and the coupling mixing angle θ (Eq. (8)) instead of $\sigma_{\text{SD}}^p(0)$ and $\sigma_{\text{SD}}^n(0)$. With these definitions the SD WIMP-proton and WIMP-neutron cross sections have the form $\sigma_{\text{SD}}^p = \sigma_{\text{SD}} \cdot \cos^2 \theta$ and $\sigma_{\text{SD}}^n = \sigma_{\text{SD}} \cdot \sin^2 \theta$.

In Fig. 4 the WIMP-nucleon spin and scalar mixed couplings allowed by the annual modulation signature from the 100-kg DAMA/NaI experiment are shown inside the shaded regions. The regions from [13, 14] in the $(\xi\sigma_{\text{SI}}, \xi\sigma_{\text{SD}})$ space for $40 \text{ GeV} < m_{\text{WIMP}} < 110 \text{ GeV}$ cover spin-scalar mixing coupling for the proton ($\theta = 0$ case of [13, 14], left panel) and spin-scalar mixing coupling for the neutron ($\theta = \pi/2$, right panel). From nuclear physics one has for the proton spin dominated ^{23}Na and ^{127}I $\frac{\langle \mathbf{S}_n \rangle}{\langle \mathbf{S}_p \rangle} < 0.1$ and $\frac{\langle \mathbf{S}_n \rangle}{\langle \mathbf{S}_p \rangle} < 0.02 \div 0.23$, respectively. For $\theta = 0$ the DAMA WIMP-proton spin constraint is the severest one due to the p-oddness of the I target (see Fig. 2).

In the right panel of Fig. 4 we present the exclusion curve (dashed line) for the WIMP-neutron spin coupling from the odd-neutron isotope ^{129}Xe obtained under the mixed coupling assumptions [14] from the DAMA-LiXe (1998) experiment [49, 50, 51]. For the DAMA NaI detector the $\theta = \pi/2$ means no $\langle \mathbf{S}_p \rangle$ contribution at all. Therefore, in this case DAMA gives the subdominant $\langle \mathbf{S}_n \rangle$ contribution alone, which could be compared further with the dominant $\langle \mathbf{S}_n \rangle$ contribution in ^{73}Ge .

The scatter plots in Fig. 4 give σ_{SI}^p as a function of σ_{SD}^p (left panel) and σ_{SD}^n (right panel) calculated in the effMSSM [17]. Filled circles (green) correspond to the relic neutralino density $0.0 < \Omega_\chi h_0^2 < 1.0$, squares (red) correspond to the subdominant relic neutralino contribution $0.002 < \Omega_\chi h_0^2 < 0.1$ and triangles (black) correspond to the WMAP density constraint $0.094 < \Omega_\chi h_0^2 < 0.129$ [52, 53].

The constraints on the SUSY parameter space within the mixed coupling framework in Fig. 4 are in general much stronger in comparison with the traditional approach based on the one-coupling dominance (Figs. 1, 2 and 3).

It follows from Fig. 4 that when the LSP is the subdominant DM particle (squares in the figure), SD WIMP-proton and WIMP-neutron cross sections at a level of $3 \div 5 \cdot 10^{-3}$ pb are allowed, but the WMAP relic density constraint (triangles) together with the DAMA restrictions leaves only $\sigma_{\text{SD}}^{p,n} < 3 \cdot 10^{-5}$ pb without any visible reduction of allowed values for σ_{SI}^p . In general, according to the DAMA restrictions, very small SI cross sections are completely excluded, only $\sigma_{\text{SI}}^p > 3 \div 5 \cdot 10^{-7}$ pb are allowed. As to the SD cross section, the situation is not clear, because for the allowed values of the SI contribution the SD DAMA sensitivity did not yet reach the calculated upper bound for the SD LSP-proton cross section of $5 \cdot 10^{-2}$ pb (for the current nucleon spin structure from [54]).

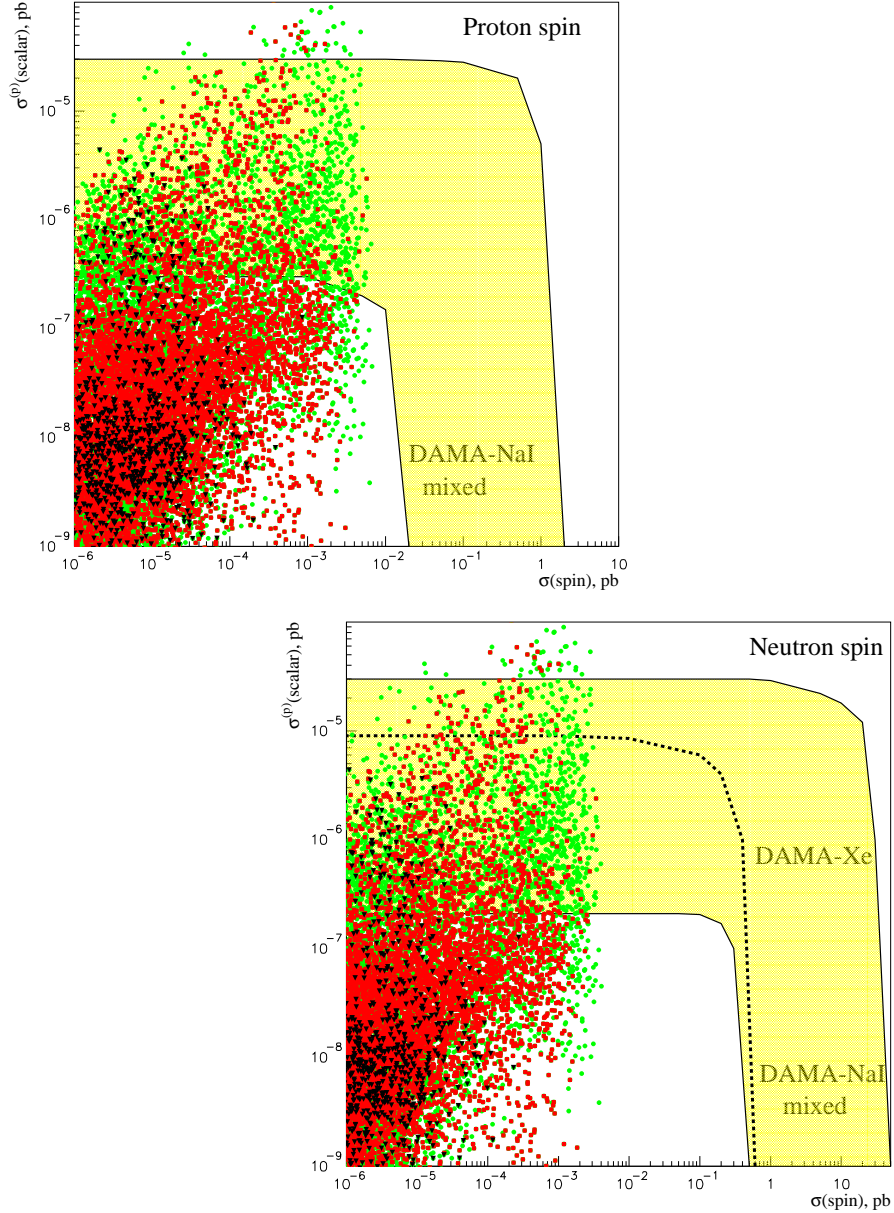


Fig. 4. The DAMA-NaI allowed region from the WIMP annual modulation signature in the $(\xi\sigma_{\text{SI}}, \xi\sigma_{\text{SD}})$ space for $40 < m_{\text{WIMP}} < 110$ GeV [13, 14]. The left panel corresponds to the dominating (in ^{127}I) SD WIMP-proton coupling alone ($\theta = 0$) and the right panel corresponds to the subdominating SD WIMP-neutron coupling alone ($\theta = \pi/2$). The scatter plots give correlations between σ_{SI}^p and σ_{SD} in the effMSSM ($\xi = 1$ is assumed) for $m_\chi < 200$ GeV [17]. In the right panel the DAMA liquid xenon exclusion curve from [14] is given (dashed line). From [17].

4 The mixed couplings case for high-spin ^{73}Ge

There are many measurements with p-odd nuclei and there is a lack of data for n-odd nuclei, i.e. for σ_{SD}^n . From our point of view this lack of σ_{SD}^n measurements can be filled with new data expected from the HDMS experiment with the high-spin isotope ^{73}Ge [55]. This isotope looks with a good accuracy like an almost pure n-odd group nucleus with $\langle \mathbf{S}_n \rangle \gg \langle \mathbf{S}_p \rangle$ (Table 1). The variation in $\langle \mathbf{S}_p \rangle$ and $\langle \mathbf{S}_n \rangle$ in the table reflects the level of inaccuracy and complexity of the current nuclear structure calculations.

Table 1. All available calculations in different nuclear models for the zero-momentum spin structure (and predicted magnetic moments μ) of the ^{73}Ge nucleus. The experimental value of the magnetic moment given in the brackets is used as input in the calculations.

$^{73}\text{Ge} (G_{9/2})$	$\langle \mathbf{S}_p \rangle$	$\langle \mathbf{S}_n \rangle$	μ (in μ_N)
ISPSM, Ellis-Flores [15, 56]	0	0.5	-1.913
OGM, Engel-Vogel [21]	0	0.23	$(-0.879)_{\text{exp}}$
IBFM, Iachello at al. [57] and [11]	-0.009	0.469	-1.785
IBFM (quenched), Iachello at al. [57] and [11]	-0.005	0.245	$(-0.879)_{\text{exp}}$
TFFS, Nikolaev-Klapdor-Kleingrothaus, [58]	0	0.34	—
SM (small), Ressel at al. [11]	0.005	0.496	-1.468
SM (large), Ressel at al. [11]	0.011	0.468	-1.239
SM (large, quenched), Ressel at al. [11]	0.009	0.372	$(-0.879)_{\text{exp}}$
“Hybrid” SM, Dimitrov at al. [59]	0.030	0.378	-0.920

In the mixed spin-scalar coupling case the direct detection rate (1) in ^{73}Ge integrated over recoil energy from the threshold energy, ϵ , to the maximal energy, ε , is a sum of the SD and SI contributions:

$$R(\epsilon, \varepsilon) = \alpha(\epsilon, \varepsilon, m_\chi) \sigma_{\text{SI}}^p + \beta(\epsilon, \varepsilon, m_\chi) \sigma_{\text{SD}}; \quad (12)$$

$$\alpha(\epsilon, \varepsilon, m_\chi) = N_T \frac{\rho_\chi M_A}{2m_\chi \mu_p^2} A^2 A_{\text{SI}}(\epsilon, \varepsilon),$$

$$\beta(\epsilon, \varepsilon, m_\chi) = N_T \frac{\rho_\chi M_A}{2m_\chi \mu_p^2} \frac{4}{3} \frac{J+1}{J} (\langle \mathbf{S}_p^A \rangle \cos \theta + \langle \mathbf{S}_n^A \rangle \sin \theta)^2 A_{\text{SD}}(\epsilon, \varepsilon);$$

$$A_{\text{SI,SD}}(\epsilon, \varepsilon) = \frac{\langle v \rangle}{\langle v^2 \rangle} \int_\epsilon^\varepsilon dE_R F_{\text{SI,SD}}^2(E_R) I(E_R). \quad (13)$$

To estimate the event rate (12) one should know a number of quite uncertain astrophysical and nuclear structure parameters as well as the precise characteristics of the experimental setup (see, for example, the discussions in [13, 60]).

We neglect the subdominant contribution from the WIMP-proton spin coupling proportional to $\langle \mathbf{S}_p^A \rangle$ for ^{73}Ge . We consider only a simple spherically

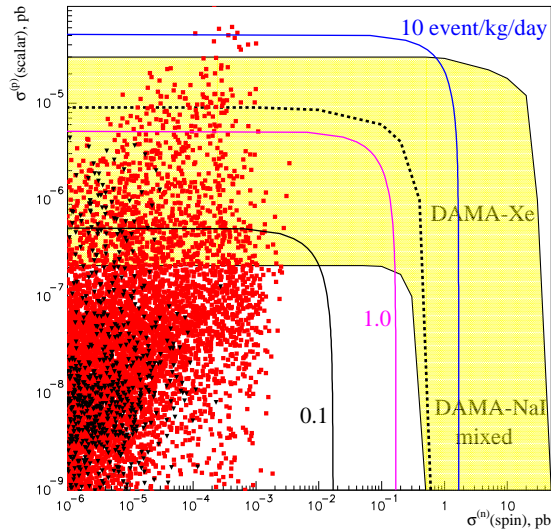


Fig. 5. Solid lines (marked with numbers of $R(15, 50)$ in events/kg/day) show the sensitivities of the HDMS setup with ^{73}Ge within the framework of mixed SD WIMP-neutron and SI WIMP-nucleon couplings. The DAMA-NaI region for the subdominant SD WIMP-neutron coupling ($\theta = \pi/2$) is from Fig. 4. Scatter plots give correlations between σ_{SI}^p and σ_{SD}^n in the effMSSM for $m_\chi < 200$ GeV [17]. Squares (red) correspond to the subdominant relic neutralino contribution $0.002 < \Omega_\chi h_0^2 < 0.1$ and triangles (black) correspond to the WMAP relic neutralino density $0.094 < \Omega_\chi h_0^2 < 0.129$. The dashed line from [14] shows the DAMA-LiXe (1998) exclusion curve for $m_{\text{WIMP}} = 50$ GeV. From [17].

symmetric isothermal WIMP velocity distribution [20, 61] and do not go into details of any possible and in principle important uncertainties (and/or modulation effects) of the Galactic halo WIMP distribution [62]–[67]. For simplicity we use the Gaussian scalar and spin nuclear form-factors from [56, 68]. With formulas (12) we performed a simple estimation of prospects for the DM search and SUSY constraints with the high-spin ^{73}Ge detector HDMS taking into account the available results from the DAMA-NaI and LiXe experiments [13, 25, 26, 49, 50, 51].

The Heidelberg Dark Matter Search (HDMS) experiment uses a special configuration of two Ge detectors to efficiently reduce the background [69]. From the first preliminary results of the HDMS experiment with the inner HPGe crystal of enriched ^{73}Ge [55] we can estimate the current background event rate $R(\epsilon, \epsilon)$ integrated here from the “threshold” energy $\epsilon = 15$ keV to the “maximal” energy $\epsilon = 50$ keV. We obtain $R(15, 50) \approx 10$ events/kg/day. A substantial improvement of the background (up to an order of magnitude) is further expected for the setup in the Gran Sasso Underground Laboratory. In Fig. 5 solid lines for the integrated rate $R(15, 50)$ marked with

numbers 10, 1.0 and 0.1 (in events/kg/day) present our exclusion curves for $m_{\text{WIMP}} = 70$ GeV expected from the HDMS setup with ^{73}Ge within the framework of the mixed SD WIMP-neutron and SI WIMP-nucleon couplings. Unfortunately, the current background index for HDMS is not yet optimized, and the relevant exclusion curve (marked with 10 events/kg/day) has almost the same strength to reduce σ_{SD}^n as the dashed curve from the DAMA experiment with liquid Xe [14] obtained for $m_{\text{WIMP}} = 50$ GeV (better sensitivity is expected with HDMS for $m_{\text{WIMP}} < 40$ GeV). However, both experiments lead to some sharper restriction for σ_{SD}^n than obtained by DAMA (see Fig. 5). An order of magnitude improvement of the HDMS sensitivity (curve marked with 1.0) will supply us with the best exclusion curve for the SD WIMP-neutron coupling, but this sensitivity is not yet enough to reach the calculated upper bound for σ_{SD}^n . This sensitivity also could reduce the upper bound for the SI WIMP-proton coupling σ_{SI}^p to a level of 10^{-5} pb. Nevertheless, only an *additional* about-one-order-of-magnitude HDMS sensitivity improvement is needed to obtain decisive constraints on σ_{SI}^p as well as on σ_{SD}^n . In this case only quite narrow bounds for these cross sections will be allowed (below the curve marked by 0.1 and above the lower bound of the DAMA-NaI mixed region).

5 Conclusion

In this paper we argue that potentially misleading discrepancies between the results of different dark matter search experiments (for example, DAMA vs CDMS and EDELWEISS) as well as between the data and the SUSY calculations can be avoided by using the mixed spin-scalar coupling approach, where the spin-independent and spin-dependent WIMP-nucleon couplings are a priori considered to be *both* non-zero. There is generally some possible incorrectness in the direct comparison of the exclusion curves for the WIMP-proton(neutron) spin-dependent cross section obtained with and without the non-zero WIMP-neutron(proton) spin-dependent contribution.

On the other hand, nuclear spin structure calculations show that usually one, WIMP-proton $\langle \mathbf{S}_p^A \rangle$ or WIMP-neutron $\langle \mathbf{S}_n^A \rangle$, nuclear spin dominates and the WIMP-proton and WIMP-neutron effective couplings a_n and a_p are of the same order of magnitude. Therefore at the current level of accuracy it looks safe to neglect subdominant WIMP-nucleon contributions when one analyses the data from non-zero-spin targets. The clear “old” odd-group-based approach to the analysis of the SD data from experiments with heavy enough targets (for example, Ge-73) is still quite suitable.

Furthermore the above-mentioned incorrectness concerns to a great extent the direct comparison of spin-dependent exclusion curves obtained with and without non-zero spin-independent contributions [13, 26]. Taking into account both spin couplings a_p and a_n but ignoring the scalar coupling c_0 , one can easily arrive at a misleading conclusion especially for not very light target

nuclei when it is not obvious that (both) spin couplings dominate over the scalar one.

To be consistent, one has to use a mixed spin-scalar coupling approach as for the first time proposed by the DAMA collaboration [25, 13, 26]. We applied the spin-scalar coupling approach to estimate future prospects of the HDMS experiment with the neutron-odd group high-spin isotope ^{73}Ge . Although even at the present accuracy the odd-neutron nuclei ^{73}Ge and ^{129}Xe lead to somewhat sharper restrictions for σ_{SD}^n than obtained by DAMA, we found that the current accuracy of measurements with ^{73}Ge (as well as with ^{129}Xe and NaI) has not yet reached a level which allows us to obtain new decisive constraints on the SUSY parameters.

This investigation was partly supported by the RFBR (Project 02-02-04009).

References

1. G. Jungman, M. Kamionkowski, and K. Griest, *Phys. Rept.* **267** (1996) 195–373.
2. J. D. Lewin and P. F. Smith, *Astropart. Phys.* **6** (1996) 87–112.
3. P. F. Smith and J. D. Lewin, *Phys. Rept.* **187** (1990) 203.
4. V. A. Bednyakov and H. V. Klapdor-Kleingrothaus, *Phys. Atom. Nucl.* **62** (1999) 966–974.
5. V. A. Bednyakov, S. G. Kovalenko, and H. V. Klapdor-Kleingrothaus, *Phys. Atom. Nucl.* **59** (1996) 1718–1727.
6. V. A. Bednyakov, H. V. Klapdor-Kleingrothaus, and S. G. Kovalenko, *Phys. Rev.* **D55** (1997) 503–514.
7. V. A. Bednyakov, S. G. Kovalenko, H. V. Klapdor-Kleingrothaus, and Y. Ramachers, *Z. Phys.* **A357** (1997) 339–347.
8. V. A. Bednyakov, H. V. Klapdor-Kleingrothaus, and S. Kovalenko, *Phys. Rev.* **D50** (1994) 7128–7143.
9. J. Engel, *Phys. Lett.* **B264** (1991) 114–119.
10. J. Engel, S. Pittel, and P. Vogel, *Int. J. Mod. Phys.* **E1** (1992) 1–37.
11. M. T. Ressell et al., *Phys. Rev.* **D48** (1993) 5519–5535.
12. M. T. Ressell and D. J. Dean, *Phys. Rev.* **C56** (1997) 535–546.
13. R. Bernabei et al., *Riv. Nuovo Cim.* **26** (2003) 1–73.
14. R. Bernabei et al., *Phys. Lett.* **B509** (2001) 197–203.
15. J. R. Ellis and R. A. Flores, *Nucl. Phys.* **B307** (1988) 883.
16. V. A. Bednyakov, H. V. Klapdor-Kleingrothaus, and S. G. Kovalenko, *Phys. Lett.* **B329** (1994) 5–9.
17. V. A. Bednyakov and H. V. Klapdor-Kleingrothaus, *Phys. Rev.* **D70**, (2004) 096006.
18. V. A. Bednyakov and F. Simkovic, *Phys. of Particles and Nuclei*, **36** (2004) 131.
19. M. W. Goodman and E. Witten, *Phys. Rev.* **D31** (1985) 3059.
20. A. K. Drukier, K. Freese, and D. N. Spergel, *Phys. Rev.* **D33** (1986) 3495–3508.

21. J. Engel and P. Vogel, Phys. Rev. **D40** (1989) 3132–3135.
22. D. S. Akerib *et al.* [CDMS Collaboration], Phys. Rev. Lett. **93**, 211301 (2004).
23. V. Sanglard, astro-ph/0406537.
24. D. R. Tovey, R. J. Gaitskell, P. Gondolo, Y. Ramachers, and L. Roszkowski, Phys. Lett. **B488** (2000) 17–26.
25. R. Bernabei *et al.*, Phys. Lett. **B480** (2000) 23–31.
26. R. Bernabei *et al.*, astro-ph/0311046.
27. G. Chardin, astro-ph/0411503.
28. A. Kurylov and M. Kamionkowski, Phys. Rev. **D69** (2004) 063503.
29. C. J. Copi and L. M. Krauss, Phys. Rev. **D63** (2001) 043507.
30. C. J. Copi and L. M. Krauss, Phys. Rev. **D67** (2003) 103507.
31. M. Drees, hep-ph/0410113.
32. G. Gelmini and P. Gondolo, hep-ph/0405278.
33. C. Savage, P. Gondolo and K. Freese, astro-ph/0408346.
34. V. A. Bednyakov, hep-ph/0310041.
35. V. A. Bednyakov and H. V. Klapdor-Kleingrothaus, Phys. Rev. **D62** (2000) 043524.
36. V. Mandic, A. Pierce, P. Gondolo, and H. Murayama, hep-ph/0008022, LBNL-46431, LBL-46431, UCB-PTH-00-23, MPI-PHT-2000-26.
37. L. Bergstrom and P. Gondolo, Astropart. Phys. **5** (1996) 263–278, also in Proc. of 4th Int. Symposium on Sources and Detection of Dark Matter in the Universe (DM 2000), Marina del Rey, California, 23-25 Feb 2000, ed. D. Cline, Springer (2001) 177-181.
38. P. Gondolo, hep-ph/0005171.
39. V. A. Bednyakov and H. V. Klapdor-Kleingrothaus, Phys. Rev. **D59** (1999) 023514.
40. L. Bergstrom, Rept. Prog. Phys. **63** (2000) 793.
41. A. Bottino, F. Donato, N. Fornengo, and S. Scopel, Phys. Rev. **D63** (2001) 125003.
42. B. Ahmed *et al.*, Astropart. Phys. **19** (2003) 691–702.
43. K. Miuchi *et al.*, Astropart. Phys. **19** (2003) 135–144.
44. F. Giuliani and T. Girard, astro-ph/0311589.
45. F. Giuliani, hep-ph/0404010.
46. A. Takeda *et al.*, Phys. Lett. **B572** (2003) 145–151.
47. P. C. Divari, T. S. Kosmas, J. D. Vergados, and L. D. Skouras, Phys. Rev. **C61** (2000) 054612.
48. V. A. Bednyakov, Phys. Atom. Nucl. **66** (2003) 490–493.
49. R. Bernabei *et al.*, Nucl. Phys. Proc. Suppl. **110** (2002) 88–90.
50. R. Bernabei *et al.*, Phys. Lett. **B436** (1998) 379–388.
51. R. Bernabei *et al.*, Nucl. Instrum. Meth. **A482** (2002) 728–743.
52. D. N. Spergel *et al.*, Astrophys. J. Suppl. **148** (2003) 175.
53. C. L. Bennett *et al.*, Astrophys. J. Suppl. **148** (2003) 1.
54. J. R. Ellis, A. Ferstl, and K. A. Olive, Phys. Lett. **B481** (2000) 304–314.
55. H. V. Klapdor-Kleingrothaus *et al.*, to be Published (2005).
56. J. R. Ellis and R. A. Flores, Phys. Lett. **B263** (1991) 259–266.
57. F. Iachello, L. M. Krauss, and G. Maino, Phys. Lett. **B254** (1991) 220–224.
58. M. A. Nikolaev and H. V. Klapdor-Kleingrothaus, Z. Phys. **A345** (1993) 373–376.
59. V. Dimitrov, J. Engel, and S. Pittel, Phys. Rev. **D51** (1995) 291–295,

60. R. Bernabei et al., astro-ph/0305542, also in Proc. of 10th Int. Workshop on Neutrino Telescopes, Venice, Italy, 11-14 Mar 2003. (2003) vol. 2, 403-423.
61. K. Freese, J. A. Frieman, and A. Gould, Phys. Rev. **D37** (1988) 3388.
62. A. Kinkhabwala and M. Kamionkowski, Phys. Rev. Lett. **82** (1999) 4172–4175.
63. F. Donato, N. Fornengo, and S. Scopel, Astropart. Phys. **9** (1998) 247–260.
64. N. W. Evans, C. M. Carollo, and P. T. de Zeeuw, Mon. Not. Roy. Astron. Soc. **318** (2000) 1131.
65. A. M. Green, Phys. Rev. **D63** (2001) 043005.
66. P. Ullio and M. Kamionkowski, JHEP **03** (2001) 049.
67. J. D. Vergados, Part. Nucl. Lett. **106** (2001) 74–108.
68. J. R. Ellis and R. A. Flores, Phys. Lett. **B300** (1993) 175–182.
69. H. V. Klapdor-Kleingrothaus et al., hep-ph/0103077, and in the proc. of 3rd Int. Workshop on the Identification of Dark Matter (IDM2000), York, England, 18-22 Sep 2000, World Scientific (2001) 415-420.